FULL PAPER

DNA Hybridization-Mediated Liposome Fusion at the Aqueous Liquid Crystal Interface

*Patrick S. Noonan, Praveena Mohan, Andrew P. Goodwin, and Daniel K. Schwartz**

The prominence of receptor-mediated bilayer fusion in cellular biology motivates development of biomimetic strategies for studying fusogenic mechanisms. An approach is reported here for monitoring receptor-mediated fusion that exploits the unique physical and optical properties of liquid crystals (LC). PEG-functionalized lipids are used to create an interfacial environment capable of inhibiting spontaneous liposome fusion with an aqueous/LC interface. Then, DNA hybridization between oligonucleotides within bulk phase liposomes and a PEG-lipid monolayer at an aqueous/LC interface is exploited to induce receptor-mediated liposome fusion. These hybridization events induce strain within the liposome bilayer, promote lipid mixing with the LC interface, and consequently create an interfacial environment favoring re-orientation of the LC to a homeotropic (perpendicular) state. Furthermore, the bi-functionality of aptamers is exploited to modulate DNA hybridization-mediated liposome fusion by regulating the availability of the appropriate ligand (i.e., thrombin). Here, a LC-based approach for monitoring receptor (i.e., DNA hybridization)-mediated liposome fusion is demonstrated, liposome properties that dictate fusion dynamics are explored, and an example of how this approach may be used in a biosensing scheme is provided.

1. Introduction

Understanding how to control bilayer fusion is fundamentally and technologically important for designing synthetic gene transfer agents,[1] drug delivery strategies,[2] studying biological systems,[3] and developing diagnostic assays.[4] In particular, in vivo biomimetic strategies for studying receptor-mediated fusion have played a major role in the advancement of this field.[5] Since Rothman and coworkers first demonstrated that SNARE proteins were the minimum machinery required for inducing membrane fusion,[6] they have been widely accepted as the most efficient fusogenic receptors. Their biological origin and prevalence in cellular membranes have inspired exploration of the mechanisms that allow SNARE proteins to work with such high efficacy.[7] A common motif has been found among SNARE receptors that involve a bundle of four alpha-helices that associate upon recognition. The configuration of this quaternary structure induced strain to the associated lipid bilayers, initiating the fusogenic process.[7] Several synthetic approaches that mimic this structural motif have been developed using peptides,[8] model proteins, small molecules, and DNA in an effort to achieve efficient recognition, bilayer disruption, and content transport in vivo.[5]

In particular, DNA hybridization-mediated fusion shows promise as a reductionist system both for studying fusion mechanics and as a bio-sensing strategy.[9–11] Studies have shown that DNA can be anchored to lipid bilayers using DNA-lipid conjugates or sterol tethered DNA.[9] Uni-lamellar liposomes can therefore be prepared with such tethered oligonucleotides. When two liposomes prepared with different but complementary oligonucleotides were combined, lipid mixing assays revealed bilayer fusion. A critical requirement in these assays was that membrane anchors on complementary DNA strands were necessarily on opposite ends of the DNA (i.e. 5′ and 3′ ends).[11] In this configuration, DNA hybridization mimicked the configuration of the four helix bundle in SNARE receptors, brought the two bilayers into close proximity, strained the bilayer structure, and consequently induced efficient lipid mixing and content transport. In the alternative situation where the tethers were on the same end of the DNA, the liposomes were observed to aggregate but no lipid mixing or content transport occurred, presumably due to a lack of bilayer-bilayer proximity and strain.

Studying receptor-mediated fusion in dispersed liposomes is convenient for proof-of-concept studies but has limited capacity for advancing related technologies. Alternatively, receptor-mediated fusion with *planar* interfaces, and in particular supported lipid bilayers, has been used for quantitative high throughput studies that elucidate cellular mechanisms related to drug discovery, medical diagnostics, and biosensor development.[12] Supported lipid bilayers can be fabricated as spatially addressed microarrays capable of high throughput screening and have demonstrated value as a tool for studying a range of biochemical processes.[13] Despite their success as model systems, supported lipid bilayers possess complicating factors such as interfering effects associated with the underlying solid substrate and the necessity of complex and expensive analytical instrumentation. Thus, substrates that address some of these drawbacks

P. S. Noonan, P. Mohan, Prof. A. P. Goodwin, Prof. D. K. Schwartz
Department of Chemical and Biological Engineering
University of Colorado Boulder
Boulder, CO 80309–0424
E-mail: daniel.schwartz@colorado.edu

DOI: 10.1002/adfm.201303885

have significant value toward a better understanding of liposome fusion from a fundamental and technological perspective. Here, we used an alternate system for monitoring liposome fusion with planar interfaces that employed a soft hydrophobic interface (i.e. liquid crystals) for depositing lipid monolayers with surface anchored receptors (i.e. DNA). We anticipated that the hydrophobic nature of the LC substrate would minimally interfere with surface anchored components while also serving as a transduction element requiring only a simple optical set up for dynamic monitoring of fusogenic activity.

Liquid crystals (LCs) have become a valuable tool for monitoring interfacial phenomena at both solid and aqueous interfaces.[14] Examples include self-assembly processes,[15–17] the dynamic behavior of hydrophobic polyanions,[18,19] protein binding[20,21] and surfactant phase behavior.[22] Studies have revealed that certain surfactants (e.g. those with long hydrocarbon tails) partitioned to the hydrophobic aqueous/LC interface, at sufficient surface densities, orient calamitic LC molecules with their long axes perpendicular to the surface (homeotropic orientation).[15,17] Importantly, only surfactants with hydrocarbon chains longer than a certain threshold length were observed to induce homeotropic orientation.[17] Among this class of surfactants were saturated phospholipids, which were deposited at the aqueous/LC interface via spontaneous liposome fusion.[23] This spontaneous fusion was shown to be independent of lipid phase, and lipid/surfactant mixtures were employed to control the relative density of lipids within a monolayer at the aqueous/LC interface. Thus, spontaneous fusion of liposomes with LC interfaces has been well characterized and is readily monitored using the optical effects associated with LC re-orientation.

More recent studies have achieved specific control over interfacial LC orientational transitions by exploiting conformational changes in adsorbed biomolecules,[18,19] localizing polar molecules via coordination interactions,[24] or mediating surfactant deposition with biomolecules.[20] In one example in particular, liposome fusion was controlled at protein decorated interfaces.[20] Liposomes were prepared with biotinylated phospholipids and introduced to a streptavidin laden LC interface. Streptavidin inhibited spontaneous fusion of undecorated liposomes with the interface while also acting as a probe to detect biotin in dispersed liposomes. When biotin bound to streptavidin at the interface, liposome fusion was initiated, and a transition to homeotropic orientation was observed. This example provided a proof-of-concept for using specific binding events to deposit lipids at an aqueous/LC interface. A more universal (and potentially multiplexed) approach requires the incorporation of membrane-anchored receptors that are compatible with a generalizable interfacial environment for inhibiting spontaneous liposome fusion.

The aim of our current study was to design a system for using biomolecular interactions to induce liposome fusion. We utilized PEG-lipid laden aqueous LC interfaces, which are inherently resistant to non-specific adsorption. We hypothesized that these interfaces would inhibit spontaneous liposome fusion and provide sufficient resistance to non-specific protein adsorption to enable the detection of specific protein binding events. Oligonucleotides were anchored to bilayers within liposomes and at the aqueous/LC interface and served as receptors for mediating liposome fusion. Using this experimental system our aims were to (i) observe and characterize DNA hybridization-mediated liposome fusion via a LC reorientation, (ii) explore the liposome properties that dictate the kinetics associated with these fusion events, and (iii) demonstrate the applicability of this approach in a detection scheme utilizing aptamers.

2. Results and Discussion

2.1. Creating a Steric Barrier to Liposome Fusion

While past studies have characterized the phase behavior of polyethylene glycol (PEG) - lipids at aqueous/LC interfaces,[22] the extent to which these interfaces inhibit non-specific adsorption had not previously been determined. Thus, our first step involved characterizing DSPE-PEG and 3′chol-DNA (see Experimental Section below for details) laden aqueous/LC interfaces. When micelles comprised of DSPE-PEG and 3′chol-DNA were introduced to the aqueous phase in contact with the LC, we observed no change in the LC orientation from the native planar orientation observed at undecorated aqueous/LC interphases. This was true for PEG molecular weights ranging from 1–5 kDa (Figure S1). Thus, under the assumption that the micelles fused with the bare LC interface, one would conclude that the presence of a DSPE-PEG/3′chol-DNA monolayer was insufficient to cause a re-orientation of the LC phase. Another less likely hypothesis, however, was that the micelles did not fuse with the LC interface. As described below, the response of the interface to subsequent changes was used to test these hypotheses.

In particular, the ability of DPPC (1,2-dipalmitoyl-sn-glycero-3-phosphocholine) liposomes to fuse with the aqueous/LC interface was found to be sensitive to the presence (or absence) of a steric barrier (i.e. PEG). When DPPC liposomes were added to the aqueous phase in contact with an LC interface, a transition to homeotropic orientation occurred due to spontaneous fusion and deposition of lipids at the interface (Figure S2). The driving force for this spontaneous fusion was the relative instability of these aggregate structures. DPPC, like most other saturated phospholipids, has a packing factor close to unity.[25] These packing factors favor a planar lamellar configuration but form spherical bilayer aggregates in bulk solution to minimize the energy costs associated with open ends in planar lamellae.[25] When a hydrophobic interface was accessible, the lipids partitioned to the interface and assembled into a favorable planar monolayer configuration without ends that were exposed to an aqueous environment.

However, in the presence of an interfacial steric barrier, the proximity of the liposomes to the hydrophobic interface may be insufficient to induce spontaneous disruption of the bilayer structure. In fact, this was exactly what we observed, as illustrated in **Figure 1**, where planar LC orientation was maintained for at least 1 h after adding DPPC liposomes to the aqueous phase in contact with a DSPE-PEG/3′chol-DNA laden interface. The same behavior was observed when 3′chol-DNA was not included in the micelles used to pre-load the interface, indicating that DSPE-PEG alone was sufficient to inhibit

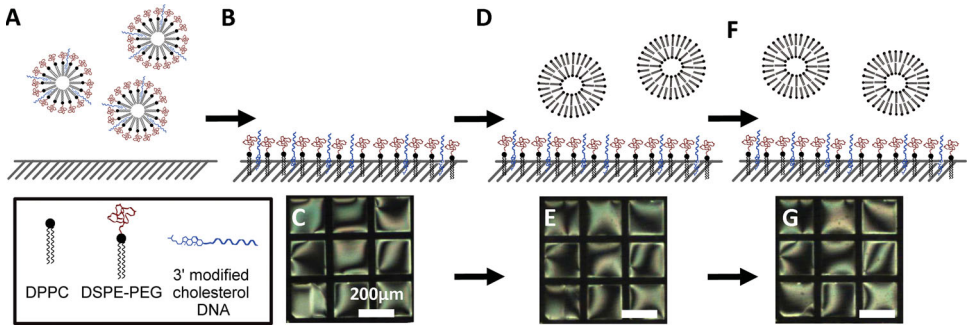

Figure 1. Inhibiting Spontaneous Liposome Fusion: (A) DSPE-PEG1k/3′chol-DNA micelles are introduced to the aqueous phase in contact with a LC interface, and (B) spontaneously fuse, (C) resulting in planar/tilted LC anchoring. (D) When DPPC liposomes are subsequently added, no change in the LC orientation is observed after (E) 1 m, or even (G) 60 m, indicative of (F) long-term fusion inhibition.

spontaneous liposome fusion. Importantly, this result verified that the DSPE-PEG micelles did in fact spontaneously fuse with the LC interface since their presence dramatically modified the interfacial fusion behavior of the DPPC liposomes. Thus, we successfully created an interfacial environment capable of inhibiting spontaneous liposome fusion.

2.2. Overcoming the Steric Barrier with DNA Hybridization

Next, we sought to utilize receptor binding (i.e. DNA hybridization) to overcome the steric barrier associated with liposome fusion to the PEG-laden LC interface. Receptor-mediated fusion involves two key steps: (1) recognition and (2) destabilization of the bilayer structure.[5] We hypothesized that if 5′chol-DNA (see Experimental Section below for details) was anchored to liposomes and introduced to a LC interface laden with complementary 3′chol-DNA, then recognition (or docking) would occur between the liposomes and the interface. To further increase the likelihood of destabilization, we used a design where the complementary DNA strands had tethers that partitioned to the same interface after hybridization (**Figure 2**A,B) and induced strain in the liposome bilayer structure. Using this approach, we successfully demonstrated receptor-mediated fusion between liposomes and the aqueous/LC interface. Specifically, a transition to homeotropic anchoring was observed (Figure 2D, and **Figure 3**A–C) upon addition of DPPC/5′chol-DNA liposomes to a DSPE-PEG1k/3′chol-DNA laden aqueous/LC interface. To verify that the lipid mixing was in fact receptor-mediated, we performed control experiments where the DNA was omitted from either the liposome or the planar interface. In both cases we found that no lipid mixing was observed (i.e. the LC orientation remained planar) (Figure 2D, and Figure 3D–I). While previous studies have revealed that DNA hybridization alone can induce LC orientational transitions,[19,26,27] the initial conditions in our system (i.e. surfactant and/or chol-DNA surface density) were insufficient for initiating these transition. Thus, the observed transition to homeotropic orientation was likely due to DNA hybridization initiating the partitioning of DPPC to the interface.

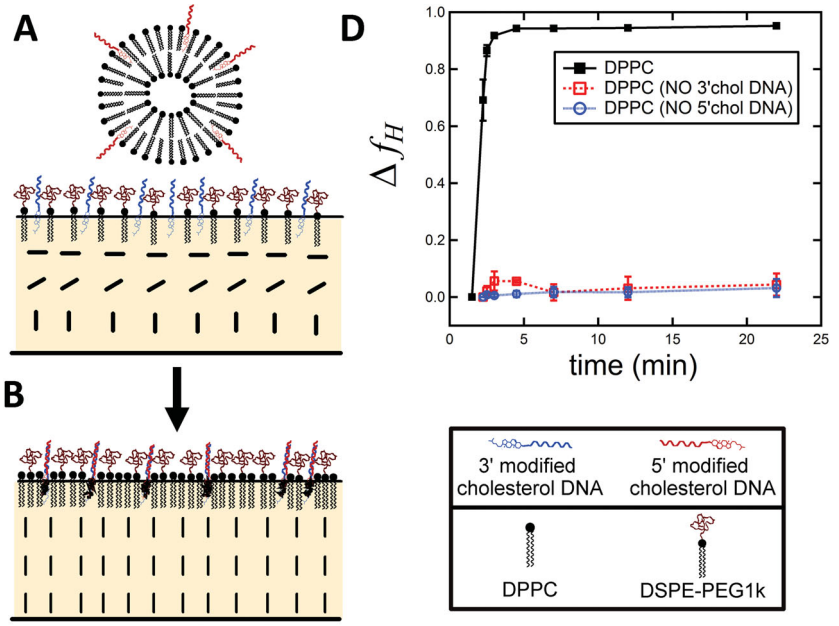

C

5′ CHOL-DNA: CHOL – 5′ TCC GTC GTG CCT TAT TTC TGA TGT CCA AAA CCA ACC ACA 3′

3′ CHOL-DNA: 5′ GTT GGT TTT GGA CAT CAG AAA TAA GGC ACG ACG GA 3′ - CHOL

Figure 2. DNA hybridization mediated fusion: (A,B) schematic representation of DNA hybridization mediated fusion where DPPC/5′chol-DNA liposomes are added above a DSPE-PEG1k/3′chol-DNA laden LC interface (A). DNA hybridization deposits DPPC at the interface (B) to induce homeotropic LC orientation. (C) DNA sequences used. (D) The fractional increase in homeotropic area (Δf_H) observed when adding liposomes ([DPPC] ≈ 4.1 mM; [5′chol-DNA] ≈ 1.6 μM; D_{pore}= 50 nm) 2 min after the initial introduction of the aqueous phase. The black curve indicates that both 5′chol-DNA and 3′chol-DNA were present in their appropriate location while the red curve is the response when 3′chol-DNA was absent and the blue curve is the response when 5′chol-DNA was absent. Error bars represent the standard error associated with the experimental data.

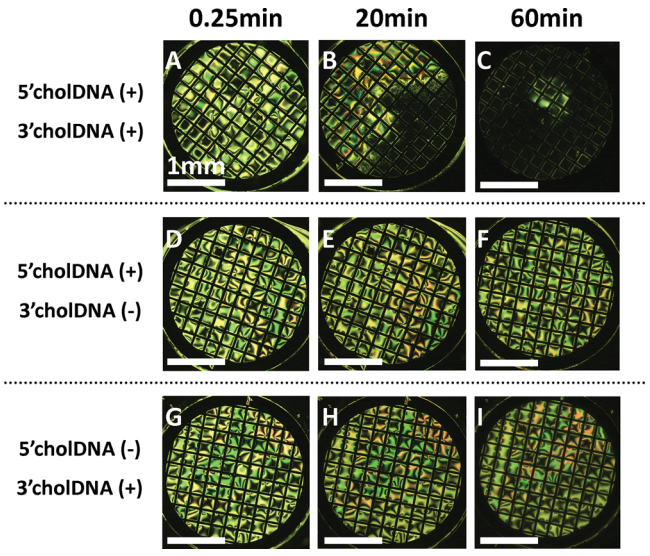

Figure 3. LC orientational transitions: polarized microscopy images of the aqueous/LC interface when either DPPC/5′cholDNA (A–C; D–F) or DPPC (G–I) liposomes were added to either a DSPE-PEG1k/3′chol-DNA (A–C; G–I) or DSPE-PEG1k (D–F) laden interface. Images were taken at 0.25 min (A,D,G), 1 min (B,E,H), and 20 min (C,F,I) after the introduction of liposomes. (note: [DPPC]≈ 4.1 mM; [5′chol-DNA] ≈ 1.6 μM; D_{pore} = 50 nm).

Consistent with the proposed mechanism, when we varied the molecular weight (MW) of the PEG group tethered to DSPE-PEG at the interface, we observed a transition to homeotropic anchoring only when the PEG MW was ≤2 kDa (Figure S1). Importantly, for each PEG MW tested, no liposome fusion was observed in the absence of 5′chol-DNA. These results suggested that when PEG groups were too large, the steric barrier was too great, consequently hindering either DNA hybridization or bilayer rupture. Also, when we varied the liposome size by extruding them through membranes with various pore sizes we observed no significant change in the fusion kinetics with liposome diameter (Figure S3). This suggested that given the fast kinetics observed, an increase in the liposome mobility (smaller liposomes) or available lipids per liposome (larger liposomes) had an insignificant effect on the rate of lipid mixing.

To better understand the effects of DNA coverage on receptor-mediated fusion kinetics we systematically varied the 5′chol-DNA content of the liposomes (see **Figure 4**). Previous studies have shown that an increased coverage of DNA on unilamellar liposomes increased the kinetics of fusion between dispersed liposomes possessing complementary oligonucleotides.[10] However, these studies addressed only a relatively narrow regime of DNA coverage and did not address the potential inhibition of fusion that could occur due to electrostatic repulsion between liposomes at high DNA coverage. As shown in Figure 4, we found that the rate of fusion was non-monotonic with respect to the DPPC:5′chol-DNA ratio. In the regime of high DNA content we observed no indication of fusion (i.e. change in LC tilt angle) on the time scales of the experiment, indicating complete inhibition of fusion. In this case, the electrostatic repulsion may have been so great that the probability of a hybridization event was insufficient to induce liposome fusion. At low 5′chol-DNA coverage we also saw a slower rate of lipid mixing, but the fusion

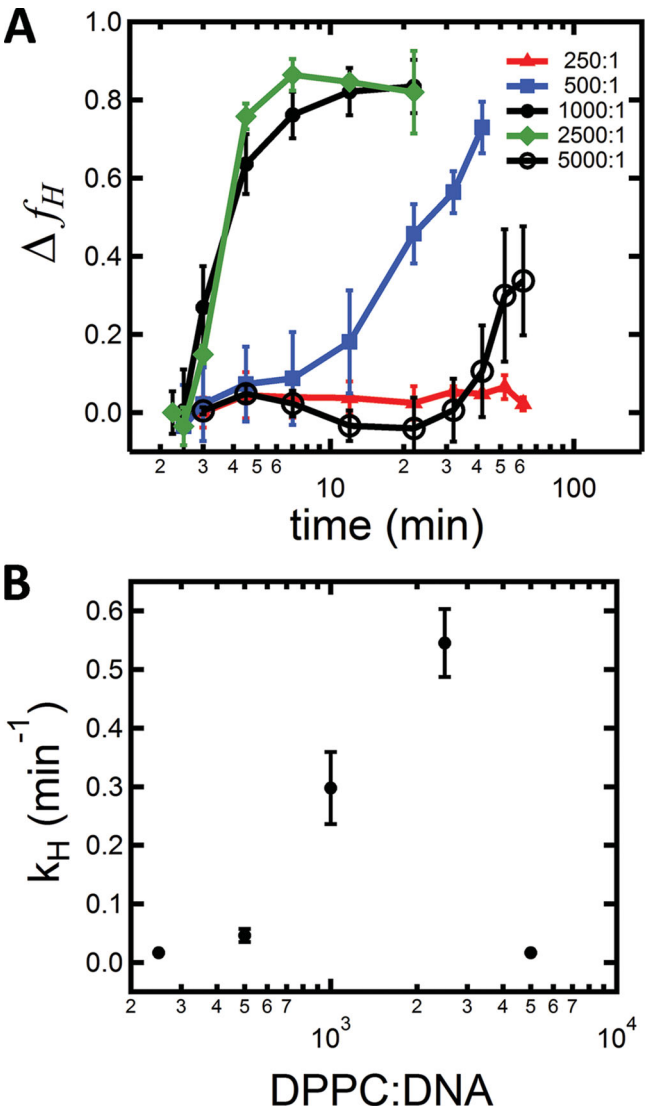

Figure 4. 5′chol-DNA coverage: (A) The fractional increase in homeotropic coverage observed at varying DPPC:5′chol-DNA ratios. (B) The effective rate constant (k_H) which represents the inverse of the time required to reach 50% homeotropic coverage (upper limit = 60 m) as interpolated from the data. (note: [DPPC] ≈ 4.1 mM; [5′chol-DNA] ≈ 1.6 μM; D_{pore} = 400 nm).

was not completely inhibited (Figure 4A). Here, we speculated that hybridization was still able to proceed but, because of the low surface density of DNA, the probability of DNA hybridization events was significantly decreased. These experiments provided insight into how electrostatics and DNA density were dictating the fusion dynamics in our system and provided us with an optimal range to use for maximizing fusion kinetics.

2.3. Molecular Sensing Using DNA Hybridization-Mediated Fusion

Finally, we performed experiments that demonstrated how this type of DNA hybridization mediated-fusion could be exploited for molecular sensing. In particular we incorporated aptamers

into the detection scheme so we could detect the presence of the protein thrombin. Aptamers are nucleic acids that are synthetically evolved using the SELEX (systematic evolution of ligands by exponential enrichment) process to bind to a specific target molecule (e.g. small molecules, antibodies, proteins).[28,29] They have become attractive as probes for multiplexed based assays due to the high sensitivity and specificity with which they bind to their respective target.[30] Since aptamers are nucleic acids, studies have shown that they possess a degree of bi-functionality, since they bind to complementary DNA strands, via hybridization, and appropriate molecular targets. Often, aptamers bound with a stronger affinity to their respective ligand than to a complementary DNA sequence.[31] We exploited this phenomenon to control the DNA hybridization mediated fusion described above by the presence of the appropriate ligand.

The detection scheme is schematically illustrated in **Figure 5**. Liposomes were prepared with 5′chol-DNA and exposed to a complementary aptamer sequence that bound to the protein thrombin.[32] In the absence of thrombin the aptamer was hybridized to 5′chol-DNA, and effectively blocked hybridization between the liposomes and surface-anchored DNA strands (Figure 5A,B). However, when liposomes were exposed to sufficiently high concentrations of thrombin (Figure 5C), the aptamer was expected to dissociate from 5′chol-DNA due to competitive binding with thrombin, freeing the liposome-anchored 5′chol-DNA to hybridize with surface anchored 3′chol-DNA (Figure 5D) and promoting fusion. Thus we postulated that the exposure of liposomes prepared with 5′chol-DNA and aptamer to a DSPE-PEG/3′chol-DNA laden interface would fail to induce a transition to homeotropic orientation. But such a transition was hypothesized to occur in the presence of thrombin.

Figure 6 summarizes the results of experiments testing these hypotheses as a function of thrombin concentration. Specifically, a transition to homeotropic orientation was observed only when DPPC/5′chol-DNA/aptamer liposomes were added to a DSPE-PEG1k/3′chol-DNA laden aqueous/LC interface in the presence of sufficiently high concentrations of thrombin. When the thrombin concentration was less than ~110 nM, no increase in homeotropic coverage was observed after ~60 min, while at concentrations in the range 221–831 nM we saw a transition to nearly 100% homeotropic coverage. Assuming a simple competitive binding model with disassociation constants of 200 nM and 196 nM for aptamer-thrombin and aptamer-DNA binding respectively,[32,33] we calculated that ~14% of the aptamer was bound to thrombin at [thrombin]≈220nM. This correlates with ~44% of the 5′chol-DNA being free to undergo hybridization with surface anchored DNA, providing some insight into the fundamental sensitivity of the system. Dose-response measurements were taken for up to ~1 h after addition of liposomes and no increase in homeotropic coverage was observed at low thrombin concentrations. However, when monitoring this system for longer times (>4 h) we observed a slow transition to homeotropic even in the absence of thrombin. We speculate that this behavior was due to the dynamic behavior of DNA duplexes, in particular to the fact that the aptamer and 5′chol-DNA existed in dynamic equilibrium. Thus, for short periods of time, and at relatively low probability, the 5′chol-DNA may have been unblocked by aptamer, creating a small but finite probability for 5′chol-DNA/3′chol-DNA hybridization. The cumulative effect of these low probability events were observed because once they occured, they were essentially irreversible since the lipids used in our study had an effectively insurmountable energy barrier to desorption. However, the rate of these "false negative" events was sufficiently low to monitor the specific fusogenic activity mediated by aptamer-ligand binding.

3. Conclusions

While LC interfaces have previously been designed to detect specific proteins,[34,35] a robust detection scheme that combines protein resistant surfaces with protein recognition-mediated LC orientational transformations has yet to be realized. Previous studies have shown that macromolecular proteins readily adsorbed to the aqueous/LC interface, disrupted the interfacial structure associated with homeotropic orientation, and inhibited specific protein detection. Oligo-ethylene glycol laden aqueous/LC interfaces reduced non-specific protein adsorption, consequently inhibiting the proteins' ability to disrupt the homeotropic orientation associated with surfactant laden interfaces.[36] Here, we employed similar interfacial conditions to create protein-resistant surfaces within a robust detection scheme. To illustrate this point, we show that when thrombin was added during DPPC

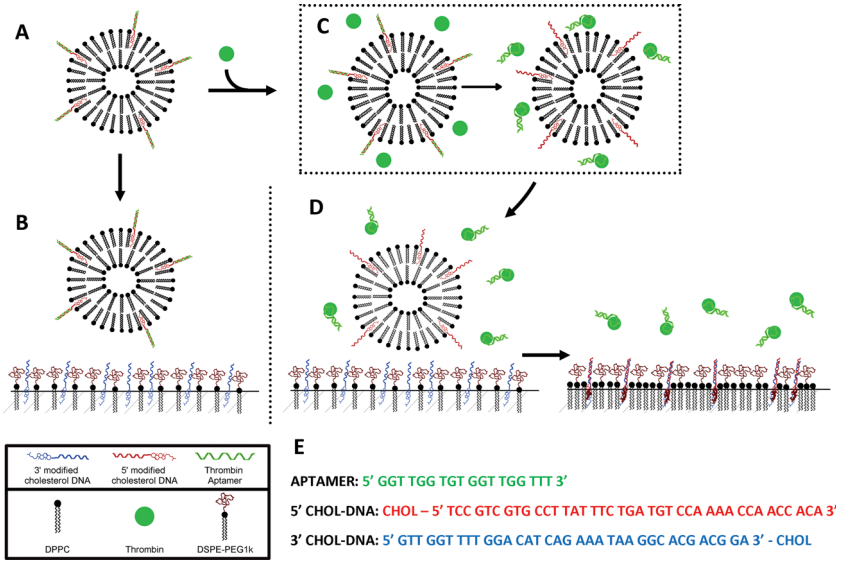

Figure 5. Schematic of Aptamer-Ligand binding mediated Liposome Fusion: DPPC (A,E) Liposomes are prepared with 5′chol-DNA and aptamer. (B) When these liposomes are added to a DSPE-PEG1k/3′chol-DNA laden LC interface fusion is inhibited since the aptamer blocks DNA hybridization. (C) If the liposomes are mixed with thrombin prior to addition, (D) it bound to the aptamer causing it to disassociate from 5′chol-DNA and (D) allowed DNA hybridization mediated fusion to proceed. (E) oligonucleotide sequences used.

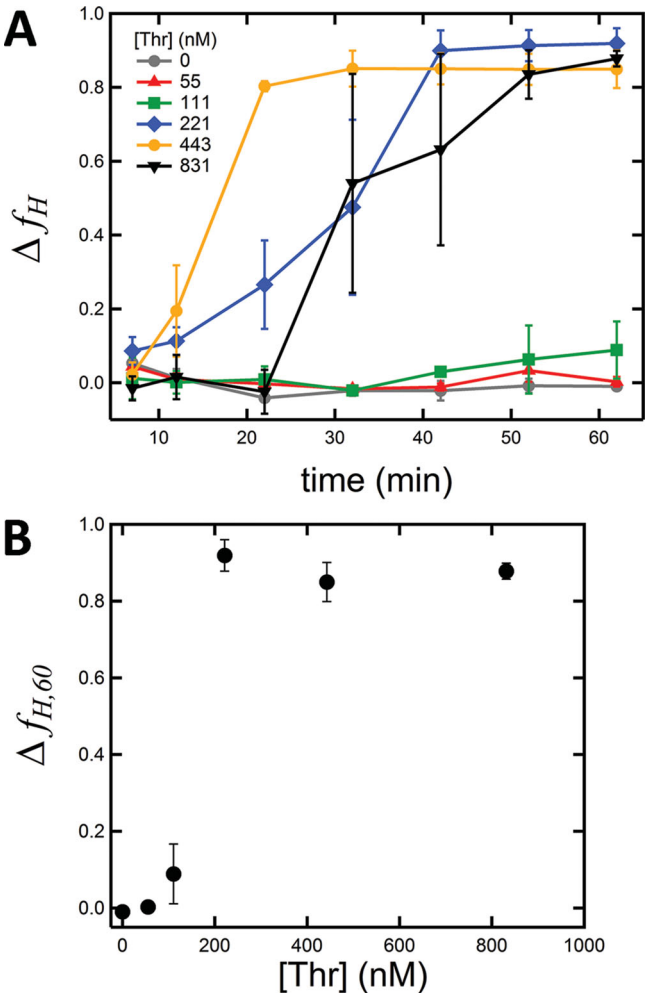

Figure 6. Thrombin Dose-Response: (A) The fractional increase in homeotropic area (f_H) observed when adding DPPC/5′chol-DNA/aptamer liposomes *a priori* incubated with varying concentrations of thrombin to a DSPE-PEG1k/3′chol-DNA laden interface (B) The fractional increase in homeotropic area 60 minutes after the introduction of liposomes ($f_{H,60}$) plotted against thrombin concentration. (note: [DPPC] ≈ 1.36 mM; [5′chol-DNA] ≈ [aptamer] ≈ 0.85 μM; D_{pore} = 100 nm).

liposome fusion, protein adsorption to the interface inhibited the extent to which DPPC was able to induce a transition to homeotropic orientation (Figure S2). Thus, in our detection scheme, if our surfaces had no resistance to non-specific protein adsorption, we would not have been able to observe a transition to homeotropic orientation. The observation of nearly 100% homeotropic coverage, even in the presence of relatively high concentrations of thrombin (Figure 6), was evidence of interfacial conditions that not only inhibited spontaneous liposome fusion but also inhibited the non-specific adsorption of proteins. While decreased fusion kinetics were observed at thrombin concentrations > 800 nM (likely due to thrombin interfering with the fusion dynamics), a complete transition was still observed, suggesting that the PEG sufficiently inhibited non-specific protein adsorption even at high thrombin concentrations. Thus, we have demonstrated that DNA hybridization mediated fusion at protein resistant surfaces was exploited for detection of macromolecular proteins. Since the materials required for these experiments were relatively inexpensive (requiring only a simple optical set-up) and responded rapidly ($t_{50\%}$ < 1 min), this approach also shows promise for high throughput screening of fusogenic receptors and aptamer-based biosensing. Future work will involve extending this approach toward detecting other types of receptor mediated liposome fusion (e.g. SNARE, small molecule) and further optimizing conditions (e.g. PEG size, DNA:aptamer ratio) for advanced aptamer based bio-sensing applications (e.g. detection in complex media).

4. Experimental Section

Materials: Lipids (i.e., (1,2-distearoyl-sn-glycero-3-phosphoethanolamine-*N*-[methoxy(polyethylene glycol)-1000] (ammonium salt)) DSPE-PEG1k; (1,2-distearoyl-sn-glycero-3-phosphoethanolamine-*N*-[methoxy (polyethylene glycol)-2000] (ammonium salt)) DSPE-PEG2k; (1,2-distearoyl-sn-glycero-3-phosphoethanolamine-*N*-[methoxy(polyethylene glycol)-5000] (ammonium salt)) DSPE-PEG5k; 1,2-dipalmitoyl-sn-glycero-3-phosphocholine (DPPC)) were purchased from Avanti Polar Lipids Inc. Oligonucleotides (*5′chol-DNA*: CHOL – 5′ TCC GTC GTG CCT TAT TTC TGA TGT CCA AAA CCA ACC ACA 3′; *3′chol-DNA*: 5′ GTT GGT TTT GGA CAT CAG AAA TAA GGC ACG ACG GA 3′ – CHOL, and aptamer: 5′ GGT TGG TGT GGT TGG TTT 3′) were purchased from IDT Technologies. Thrombin from human plasma (≥1000 NIH units/mg) was purchased from Sigma-Aldrich and suspended in aqueous buffer at concentrations ranging from 3–10 μM as verified by absorption measurements at λ = 280 nm (i.e., Nanodrop 2000). A liquid crystal mixture, E7 (a mixture of three cyano-biphenyls and a cyano-terphenyl), was purchased from Merck Kga. Aqueous buffers were prepared from powder stocks of Tris-HCl (Fisher) and NaCl (Fisher) constituted at the proper concentrations in deionized water (18.2 MΩ cm) and adjusted to pH ~ 8.5 by addition of 0.1 M NaOH. Octadecyltriethoxysilane was purchased from Gelest Inc. and deposited onto soda-lime glass microscope slides (Fisher) according to the procedure outlined below. Electron microscopy grids (CP-100) were purchased from Electron Microscopy Sciences. Silicone isolators were purchased from Grace Bio Labs and were used as wells to contain the aqueous phase above the LC interface.

Liposome Preparation: Liposomes were prepared by first dissolving a known mass of the appropriate lipid in chloroform. Chloroform was then removed by rotary evaporation at ~55 °C with a rotation speed of 200–250 rpm to obtain a homogenous lipid film. The film was subsequently solvated in an aqueous buffer (10 mM Tris, 100 mM NaCl, pH ~ 8.5) at [lipid] ~ 6.8 mM and incubated in a water bath at ~70 °C for 30–60 m. Once lipids were completely dispersed in aqueous buffer, we diluted the lipid solution to the desired concentration and added the applicable DNA strands at the appropriate concentrations. The lipid/DNA mixture was incubated at ~70 °C for 30–60 m to allow sufficient time to incorporate into the lipid bilayer. Finally, we sized the vesicles using a membrane extruder (Avanti Polar Lipids Inc.) with membrane pore sizes (D_{pore}) of 50, 100, or 400 nm. Liposome diameters were subsequently measured using photon correlation spectroscopy. DSPE-PEG micelles were always prepared at the same concentration by mixing DSPE-PEG (and 3′ chol-DNA when applicable) with aqueous buffer (10 mM Tris, 100 mM NaCl, pH ~ 8.5) to a final [DSPE-PEG] ≈ 40.2 μM ([3′chol-DNA] ≈ 0.85 μM) and vortexing the mixture for 30–60 s.

LC Film Preparation: Preparation of self-assembled monolayers (SAMs) of octadecyltriethoxysilane (OTES) was completed according to published procedures.[37] Briefly, glass slides were cleaned sequentially with 2% aqueous Micro-90 detergent, deionized water (18.2 MΩ cm), and piranha solution (30% aqueous H_2O_2 (Fisher Scientific) and concentrated H_2SO_4 (Fisher Scientific) 1:3, v/v) at ≈80 °C for 1 h. (*Warning: piranha reacts strongly with organic compounds and should be handled with extreme caution; do not*

store in a closed container). Piranha-cleaned microscope slides were then rinsed with deionized water (18.2 MΩ-cm) and dried under a stream of ultrapure N_2. Toluene, OTES, and n-butylamine (Fisher Scientific) (Fisher Scientific) were mixed at 200:3:1 volumetric ratios, respectively, and warmed to 60 °C. Clean and dry microscope slides were rinsed with toluene, submerged in the warm deposition solution, and incubated for 1 h at 60 °C. Following this incubation, the slides were rinsed with toluene, dried under a stream of ultrapure N_2, and stored at room temperature in a vacuum desiccator. The water contact angle (θ_C, measured via the static sessile drop method) of the prepared SAMs was verified to be >95° (indicative of strong homeotropic anchoring) using a custom-built contact angle goniometer.

Aqueous/LC interfaces were prepared by housing LC films within the pores of an electron microscopy grid. The grids were initially placed onto a solid glass substrate functionalized with an OTES self-assembled monolayer (SAM) and contained within silicone isolators. The SAM served to maintain homeotropic orientation of the LC at the solid substrate. The pores of the electron microscopy grid were then filled with E7 by pipetting ~250 nL into the grid and removing the excess via capillary action. Next, the wells were filled with ~25 µL of an aqueous solution. When depositing DSPE-PEG micelles to the interface, aqueous buffer containing the appropriate DSPE-PEG micelles were added during this initial introduction of the aqueous phase. Liposomes were subsequently added two minutes after the initial introduction of the aqueous phase by pipetting an additional 25 µL of the desired liposome mixture, mixing the solution in the wells by pipetting, then removing 25 µL to re-establish the planar air-water interface that allows for efficient imaging (note: curvature of the air-water interface caused reflections that distorted polarized light microscopy images). The LC orientation and textures were dynamically monitored between crossed polarizers using a custom built transmission microscope.

Image Analysis: Images obtained from polarized light microscopy (PLM) were analyzed using customized algorithms in the Mathematica programming environment. The region of interest was first selected using an image convolution function to find the center of the electron microscopy grid, and a constant grid diameter to select the region of interest for analysis. Next, images were binarized to obtain the fraction of dark pixels in a given image. However, this fraction of dark pixels did not directly correlate with homeotropic coverage since in-plane (i.e. azimuthal) alignment of LC molecules around point defects resulted in extinction at angles parallel or normal to the incident polarization of light. Since the surface area of LC film that experienced this extinction in our system was relatively constant we were able to circumvent this artifact by using a normalization approach. We obtained the fractional increase in homeotropic coverage (Δf_H) as a function of time within a series of images according to the following equation:

$$\Delta f_H = \frac{f_t - f_o}{1 - f_o}$$

where f_o was the fraction of dark pixels in a qualitatively planar image from the same time series and f_t was the fraction of dark pixels at time = t.

Supporting Information

Supporting Information is available from the Wiley Online Library or from the author.

Acknowledgements

This work was supported by the National Science Foundation (Award CBET-1160202), the National Institue of Health (Award NIH R00-CA153935), and the Liquid Crystal Materials Research Center (NSF/MRSEC, Award DMR-820579).

Received: November 17, 2013
Revised: December 23, 2013
Published online: February 18, 2014

[1] W.-C. Tseng, L. Huang, *Pharmaceut. Sci. Technol. Today* **1998**, *1*, 206.
[2] G. Gregoriadis, *Trends Biotechnol.* **1995**, *13*, 527.
[3] L. Shi, Q. T. Shen, A. Kiel, J. Wang, H. W. Wang, T. J. Melia, J. E. Rothman, F. Pincet, *Science* **2012**, *335*, 1355.
[4] C. Fan, N. Dave, J. LiuDNA Nanotechnology From Structure to Function, Springer, Berlin Heidelberg, **2013**, 5776.
[5] M. Ma, D. Bong, *Acc. Chem. Res.*, **2013**, *46*(12), 2988–2997.
[6] T. Weber, B. V. Zemelman, J. A. McNew, B. Westermann, M. Gmachl, F. Parlati, T. H. Sollner, J. E. Rothman, *Cell* **1998**, *92*, 759.
[7] D. Ungar, F. M. Hughson, *Annu. Rev. Cell Developmental Biol.* **2003**, *19*, 493.
[8] H. R. Marsden, N. A. Elbers, P. H. H. Bomans, N. A. J. M. Sommerdijk, A. Kros, *Angew. Chem.-Int. Ed.* **2009**, *48*, 2330.
[9] G. Stengel, R. Zahn, F. Hook, *J. Am. Chem. Soc.* **2007**, *129*, 9584.
[10] G. Stengel, L. Simonsson, R. A. Campbell, F. Hook, *J. Phys. Chem. B* **2008**, *112*, 8264.
[11] Y. H. M. Chan, B. van Lengerich, S. G. Boxer, *Biointerphases* **2008**, *3*, Fa17.
[12] E. T. Castellana, P. S. Cremer, *Surf. Sci. Rep.* **2006**, *61*, 429.
[13] H. Bayley, P. S. Cremer, *Nature* **2001**, *413*, 226.
[14] S. J. Woltman, G. D. Jay, G. P. Crawford, *Nature Mater.* **2007**, *6*, 929.
[15] J. M. Brake, N. L. Abbott, *Langmuir* **2002**, *18*, 6101.
[16] P. S. Noonan, A. Shavit, B. R. Acharya, D. K. Schwartz, *ACS Appl. Mater. Interfaces* **2011**, *3*, 4374.
[17] J. M. Brake, A. D. Mezera, N. L. Abbott, *Langmuir* **2003**, *19*, 6436.
[18] P. S. Noonan, R. H. Roberts, D. K. Schwartz, *J. Am. Chem. Soc.* **2013**, *135*, 5183.
[19] A. C. McUmber, P. S. Noonan, D. K. Schwartz, *Soft Matter* **2012**, *8*, 4335.
[20] L. N. Tan, V. J. Orler, N. L. Abbott, *Langmuir* **2012**, *28*, 6364.
[21] C.-Y. Xue, S. A. Khan, K.-L. Yang, *Adv. Mater.* **2009**, *21*, 198.
[22] M. I. Kinsinger, D. M. Lynn, N. L. Abbott, *Soft Matter* **2010**, *6*, 4095.
[23] J. M. Brake, M. K. Daschner, N. L. Abbott, *Langmuir* **2005**, *21*, 2218.
[24] H. J. VanTreeck, D. R. Most, B. A. Grinwald, K. A. Kupcho, A. Sen, M. D. Bonds, B. R. Acharya, *Sens. Actuat. B* **2011**, *158*, 104.
[25] J. N. Israelachvili, Intermolecular and Surface Forces, 3rd Ed., Elsevier, Waltham, MA **2011**.
[26] S. L. Lai, D. Hartono, K. L. Yang, *Appl. Phys. Lett.* **2009**, *95*, 153702.
[27] A. D. Price, D. K. Schwartz, *J. Am. Chem. Soc.* **2008**, *130*, 8188.
[28] A. D. Ellington, J. W. Szostak, *Nature* **1990**, *346*, 818.
[29] C. Tuerk, L. Gold, *Science* **1990**, *249*, 505.
[30] A. B. Iliuk, L. Hu, W. A. Tao, *Anal. Chem.* **2011**, *83*, 4440.
[31] R. Nutiu, Y. Li, *J. Am. Chem. Soc.* **2003**, *125*, 4771.
[32] L. C. Bock, L. C. Griffin, J. A. Latham, E. H. Vermaas, J. J. Toole, *Nature* **1992**, *355*, 564.
[33] J. SantaLucia, *Proc. Natl. Acad. Sci. USA* **1998**, *95*, 1460.
[34] J. M. Brake, M. K. Daschner, Y. Y. Luk, N. L. Abbott, *Science* **2003**, *302*, 2094.
[35] R. J. Carlton, J. T. Hunter, D. S. Miller, R. Abbasi, P. C. Mushenheim, L. Na Tan, N. L. Abbott, *Liquid Crystals Rev.* **2013**, *1*, 29–51.
[36] Z. Q. Yang, J. K. Gupta, K. Kishimoto, Y. Shoji, T. Kato, N. L. Abbott, *Adv. Funct. Mater.* **2010**, *20*, 2098.
[37] D. M. Walba, C. A. Liberko, E. Korblova, M. Farrow, T. E. Furtak, B. C. Chow, D. K. Schwartz, A. S. Freeman, K. Douglas, S. D. Williams, A. F. Klittnick, N. A. Clark, *Liq. Cryst.* **2004**, *31*, 481.